TIFR/TH/01-36
CERN/TH/01-246

# Using Tau Polarization to Sharpen up the SUGRA Signal at Tevatron

Monoranjan Guchait[a] and D.P. Roy[a,b]

[a] Theoretical Physics Division, CERN
CH-1211, Geneva 23, Switzerland
[b] Tata Institute of Fundamental Research
Homi Bhabha Road, Mumbai 400 005, INDIA

## Abstract

The most promising source of SUGRA signal at the Tevatron collider is the pair-production of electroweak gauginos, followed by their leptonic decay. In the parameter range corresponding to dominant leptonic decay of these gauginos one or more of the leptons are expected to be $\tau$ with $P_\tau \simeq +1$. This polarization can be effectively used to distinguish the signal from the background in the 1-prong hadronic decay channel of $\tau$ by looking at the fractional $\tau$-jet momentum carried by the charged prong.

The LEP limit of chargino mass $> 90$ GeV corresponds to a gluino mass $> 300$ GeV in the minimal SUGRA model [1], which puts them beyond the discovery reach of the Tevatron collider. Thus the most promising source of SUGRA signal at Tevatron seems to be the pair production of electroweak gauginos, $\tilde{W}_1^+\tilde{W}_1^-$ and $\tilde{W}_1^\pm\tilde{Z}_2$. The leptonic decays of $\tilde{W}_1$ and $\tilde{Z}_2$ into the LSP ($\tilde{Z}_1$) result in clean dilepton and trilepton final states with a significant missing-$E_T$ ($\not{E}_T$) and very little hadronic jet activity. Recently there has been a good deal of interest in these processes as the main signatures of the SUGRA model at Tevatron [2]-[5]. The parameter space of particular interest to this signature is one where the lighter (right-handed) sleptons lye below the $\tilde{W}_1$ and $\tilde{Z}_2$ masses, resulting in very large leptonic branching fractions of these gauginos. This corresponds to two regions of the SUGRA parameter space – i.e. I) $m_0$ significantly less than $m_{1/2}$ ($m_0 \sim \frac{1}{2}m_{1/2}$), implying $m_{\tilde{\ell}_R,\tilde{\tau}_R} \lesssim m_{\tilde{W}_1,\tilde{Z}_2}$ at any value of $\tan\beta$, and II) $m_0 \sim m_{1/2}$ at large $\tan\beta$, implying $m_{\tilde{\tau}_R} \lesssim m_{\tilde{W}_1,\tilde{Z}_2}$, where $\ell$ denotes electron and muon. In the 1st case one expects a $\ell^+\ell^-\tau$ signature from $\tilde{Z}_2\tilde{W}_1$ decay, since $\tilde{W}_1 \to \tau\nu_\tau\tilde{Z}_1$ via the larger L-R mixing in the $\tilde{\tau}$ sector due to the larger $\tau$ mass. In the 2nd case one expects $\tau\tau$ and $\tau\tau\tau$ signatures from $\tilde{W}_1\tilde{W}_1$ and $\tilde{Z}_2\tilde{W}_1$ decays respectively. The presence of one or more $\tau$ leptons in the final state means that the $\tau$ channel is expected to play a very important role in superparticle search at Tevatron, particularly in the minimal SUGRA model [2]-[5].

The minimal SUGRA model predicts the polarization of $\tau$ resulting from the above $\tilde{\tau}$ decay to be $= +1$ to a good approximation, as we shall see below. The purpose of this note is to use this $\tau$ polarization ($P_\tau = +1$) to sharpen the distinction between the SUSY signal and the SM background. It has been shown in the context of charged Higgs boson search in the $H^\pm \to \tau\nu$ channel that in the 1-prong hadronic $\tau$-jet the $P_\tau = +1$ signal from $H^\pm$ decay can be effectively distinguished from the $P_\tau = -1$ background from $W^\pm$ via the sharing of the jet energy between the charged pion and the accompanying neutrals [6]-[7]. This has been confirmed now by detailed simulation studies for both Tevatron and LHC. We shall use a similar strategy here to distinguish the SUSY signal from the SM background in the 1-prong hadronic $\tau$-jet channels. In particular we shall see that the $P_\tau = +1$ signal can be effectively separated from the $P_\tau = -1$ background as well as the fake $\tau$ background from QCD jets by requiring the charged track to carry $> 80\%$ of the jet energy-momentum.

We shall concentrate on the 1-prong hadronic decay channel of $\tau$, which is best suited for $\tau$ identification. It accounts for 80% of hadronic $\tau$ decay and 50% of its total decay width. The main contributors to the 1-prong hadronic decay are

$$\tau^{\pm} \rightarrow \pi^{\pm}\nu(12.5\%),\ \rho^{\pm}\nu(26\%),\ a_1^{\pm}\nu(7.5\%), \tag{1}$$

where the branching fractions for $\pi$ and $\rho$ include the small $K$ and $K^{\star}$ contributions respectively [1], which have identical polarization effects. Together they account for 90% of the 1-prong hadronic decay. The CM angular distribution of $\tau$ decay into $\pi$ or a vector meson $v$ $(= \rho, a_1)$ is simply given in terms of its polarization as

$$\frac{1}{\Gamma_\pi}\frac{d\Gamma_\pi}{d\cos\theta} = \frac{1}{2}(1 + P_\tau \cos\theta), \tag{2}$$

$$\frac{1}{\Gamma_v}\frac{d\Gamma_{vL,T}}{d\cos\theta} = \frac{\frac{1}{2}m_\tau^2, m_v^2}{m_\tau^2 + 2m_v^2}(1 \pm P_\tau \cos\theta), \tag{3}$$

where $L, T$ denote the longitudinal and transverse polarization states of the vector meson. The fraction $x$ of the $\tau$ lab. momentum carried by its decay meson (i.e. the visible momentum of the $\tau$-jet) is related to the angle $\theta$ via

$$x = \frac{1}{2}(1 + \cos\theta) + \frac{m_{\pi,v}^2}{2m_\tau^2}(1 - \cos\theta), \tag{4}$$

where we have neglected the $\tau$ mass relative to its lab. momentum (collinear approximation). It is clear from eqs. (2) - (4) that the hard part of the $\tau$-jet, which is responsible for $\tau$ identification, is dominated by $\pi, \rho_L, a_{1L}$ for the $P_\tau = +1$ signal, while it is dominated by $\rho_T, a_{1T}$ for the $P_\tau = -1$ background. The two can be distinguished by exploiting the fact that the transverse $\rho$ and $a_1$ decays favour even sharing of momentum among the decay pions, while the longitudinal $\rho$ and $a_1$ decays favour uneven sharing, where the charged pion carries either very little or most of the momentum. It is easy to derive this quantitatively for $\rho$ decay. But one has to assume a dynamical model for $a_1$ decay to get a quantitative result. We shall assume the model of ref. [8], based on conserved axial vector current approximation, which provides a good description to the $a_1 \rightarrow 3\pi$ data. A detailed account of the $\rho$ and $a_1$ decay formalisms including finite width effects can be found in [6],[9]. A simple FORTRAN code for 1-prong hadronic decay of Polarized $\tau$ based on these formalisms can be obtained from one of the authors (D.P. Roy).

As specific examples of the two regions of interest in the SUGRA parameter space mentioned above, we have chosen two points representing the cases I and II, and evaluated the corresponding SUSY spectra using the ISASUGRA code – version 7.48 [10]. The resulting $\tilde{W}_1, \tilde{Z}_2, \tilde{Z}_1$ and the slepton masses are shown in the two rows of Table 1 along with the $\tilde{\tau}$ mixing angle, where

$$\tilde{\tau}_1 = \tilde{\tau}_R \sin\theta_\tau + \tilde{\tau}_L \cos\theta_\tau. \tag{5}$$

It may be noted here that the Polarization of the $\tau$ resulting from the $\tilde{\tau}_1 \to \tau\tilde{Z}_1$ decay is

$$P_\tau \simeq \frac{4\sin^2\theta_\tau - \cos^2\theta_\tau}{4\sin^2\theta_\tau + \cos^2\theta_\tau}, \tag{6}$$

since $\tilde{Z}_1 \simeq \tilde{B}$ in the minimal SUGRA model and $\tau_R$ has twice as large a hypercharge as $\tau_L$ [11]. For the mixing angles of Table 1, $\cos\theta_\tau = 0.19(0.53)$, we get $P_\tau = 0.98(0.85)$. Hence the $\tau$ polarization is $\simeq +1$ to a good approximation over a wide range of the relevant SUGRA parameters, notably $\tan\beta$.

Table 1. The light sparticle masses of the minimal SUGRA model for (I) $m_{1/2} = 175$, $m_0 = 70$, $\tan\beta = 5$ (top row) and (II) $m_{1/2} = 160$, $m_0 = 150$, $\tan\beta = 40$ (bottom row), where all the masses are in GeV unit. For both cases $A_0 = 0$ and sign$(\mu) = +$ve.

| $\tilde{W}_1$ | $\tilde{Z}_2$ | $\tilde{Z}_1$ | $\tilde{\nu}_\ell$ | $\tilde{\ell}_L$ | $\tilde{\ell}_R$ | $\tilde{\nu}_\tau$ | $\tilde{\tau}_2$ | $\tilde{\tau}_1$ | $\cos\theta_\tau$ |
|---|---|---|---|---|---|---|---|---|---|
| 116 | 120 | 66 | 130 | 151 | 106 | 130 | 153 | 104 | 0.19 |
| 110 | 112 | 63 | 178 | 195 | 168 | 164 | 207 | 97 | 0.53 |

We have estimated the signal and background cross-sections for the above two cases using a parton level Monte Carlo programme. To simulate detector resolution we have applied Gaussian smearing on the jet and lepton $p_T$ with $(\sigma(p_T)/p_T)^2 = (0.6/\sqrt{p_T})^2 + (0.04)^2$ and $(0.15/\sqrt{p_T})^2 + (0.01)^2$ respectively. The $\not{E}_T$ is evaluated from the vector sum of the lepton and jet $p_T$ after resolution smearing. The main results for the two cases are presented below.

## I. $m_0 \sim \frac{1}{2} m_{1/2}$ ($\ell^+\ell^-\tau$ signal):

The sparticle spectrum of the top row of Table 1 imply that the dominant decay modes of $\tilde{Z}_2$ and $\tilde{W}_1$ are

$$\tilde{Z}_2 \rightarrow \ell\tilde{\ell}_R \rightarrow \ell^+\ell^-\tilde{Z}_1, \tag{7}$$

$$\tilde{W}_1 \rightarrow \nu_\tau\tilde{\tau}_1 \rightarrow \tau\nu_\tau\tilde{Z}_1, \tag{8}$$

with branching fractions $\simeq 2/3$ and 1 respectively. Thus one expects a distinctive $\ell^+\ell^-\tau$ signal accompanied by a significant $\not{E}_T$ from $\tilde{W}_1\tilde{Z}_2$ production. Moreover this signal is expected to hold over a wide range of $\tan\beta$, since the production cross-section as well as the above decay branching fractions are insensitive to this parameter. Note that the right-handed slepton masses of Table 1 are fairly close to the $\tilde{W}_1, \tilde{Z}_2$ masses due to the LEP limit on $m_{\tilde{\ell},\tilde{\tau}}$ [1]. Hence the lepton from the $\tilde{Z}_2 \rightarrow \ell\tilde{\ell}_R$ decay is expected to be relatively soft. We have therefore imposed a modest but realistic $p_T$ cut on the softer lepton. The cuts are

$$p_T^{\ell_1} > 15 \text{ GeV},\ p_T^{\ell_2} > 10 \text{ GeV}, p_T^{\tau-\text{jet}} > 15 \text{ GeV}, \not{E}_T > 20 \text{ GeV},$$

$$|\eta_{\ell_1,\ell_2,\tau-\text{jet}}| < 2.5,\ \phi_{\ell_1\ell_2} < 150^\circ,\ M_{\ell_1\ell_2} > 10 \text{ GeV and } \neq M_Z \pm 20 \text{ GeV}. \tag{9}$$

Table 2 summarises the signal and background cross-sections after these cuts, where we have included a $\tau$ identification efficiency of 50% along with a 0.5% probability of mistagging a normal hadron jet as $\tau$ [12]. The latter is a conservative assumption, since the probability of a normal hadron jet faking a 1-prong $\tau$-jet with $p_T \sim 20$ GeV has been estimated to be about 0.3% for the CDF experiment in Run-1, going up to 0.8% for the (1+3)-prongs $\tau$-jet [13].

Table 2. The signal and background cross-sections (in fb) in the $\ell\ell\tau$ channel after the cuts of eq. (9). It includes a 50% efficiency factor for $\tau$ identification along with a 0.5% probability of mistagging a normal hadron jet as $\tau$.

| Signal | Background | |
|---|---|---|
| $\tilde{W}_1\tilde{Z}_2$ | $(Z^\star/\gamma^\star)W$ | $(Z^\star/\gamma^\star)j$ |
| 27 | 0.1 | 0.04 |

Thanks to the $\not{E}_T$ and the dilepton mass and opening angle cuts, the potentially large $(Z^\star/\gamma^\star)j$ background is reduced to $\sim 0.1\%$ of the signal. We have estimated this background using a simple analytic formula for the matrix element neglecting the vector coupling of $Z$ to $\ell\bar{\ell}$. The matrix element for $(Z^\star/\gamma^\star)W$ has been evaluated using MADGRAPH [14].

Fig. 1 shows the $P_\tau = +1$ signal as a function of the fractional $\tau$-jet momentum (R) carried by the charged-prong. For comparison it also shows the corresponding distribution assuming the signal to have $P_\tau = -1$. This could be the case e.g. in some alternative SUSY model with a higgsino LSP. The complimentary shape of the two distributions, as discussed earlier, is clearly visible in this figure. The $P_\tau = +1$ signal shows the peaks at the two ends from the $\rho_L, a_{1L}$ along with the pion contribution (added to the last bin), while the $P_\tau = -1$ distribution shows the central peak due to the $\rho_T, a_{1T}$ along with a reduced pion contribution [6],[9]. The expected luminosity of 2 fb$^{-1}$ per experiment in Run-2 corresponds to $\sim 54$ signal events in the $\ell^+\ell^-\tau$ channel for each experiment without any serious SM background. Thus one can use this distribution in this case as a confirmatory test of the minimal SUGRA model.

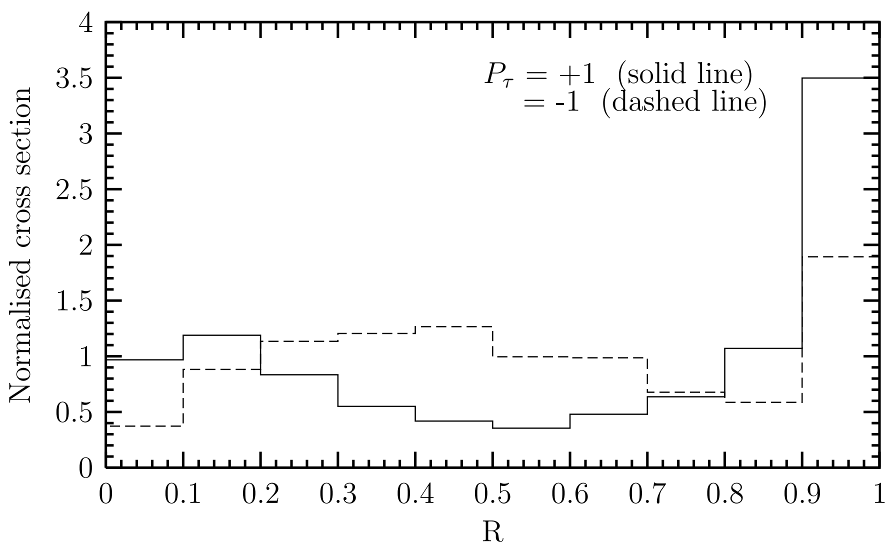


Figure 1: *The normalised $\ell\ell\tau$ signal cross-section in the 1-prong hadronic $\tau$-jet channel shown as a function of the $\tau$-jet momentum fraction (R) carried by the charged prong for $P_\tau = +1(-1)$.*

### II. $m_0 \sim m_{1/2}$ and large $\tan\beta$ ($\tau\tau$ signal):

The sparticle spectrum of the bottom row of Table 1 imply that in this case the dominant decay modes of $\tilde{Z}_2$ and $\tilde{W}_1$ are

$$\tilde{Z}_2 \to \tau\tilde{\tau}_1 \to \tau^+\tau^-\tilde{Z}_1, \tag{10}$$

$$\tilde{W}_1 \to \nu_\tau\tilde{\tau}_1 \to \tau\nu_\tau\tilde{Z}_1. \tag{11}$$

Thus one expects a $\tau\tau$ signal from $\tilde{W}_1\tilde{Z}_2$, $\tilde{W}_1\tilde{W}_1$ and $\tilde{\tau}\bar{\tilde{\tau}}$ production with $P_\tau \simeq 1$ each. The 1st process contains a 3rd $\tau$ from $\tilde{Z}_2 \to \tau\tilde{\tau}_1$, whose polarization depends on the model parameters. The contribution from the dominant ($\tilde{W}$) component of $\tilde{Z}_2$ coupling to the subdominant ($\tilde{\tau}_L$) component of $\tilde{\tau}_1$ has $P_\tau = -1$, while that from the subdominant ($\tilde{B}$) component of $\tilde{Z}_2$ coupling to the dominant ($\tilde{\tau}_R$) component of $\tilde{\tau}_1$ has $P_\tau = +1$. And it is the other way around for the higgsino component of $\tilde{Z}_2$. But in any case the $\tau$ resulting from this decay is relatively soft for the reason mentioned above and rarely survives the $\tau$-identification cut of $p_T^{\tau-\mathrm{jet}} > 15$ GeV. Therefore we shall require the identification of two $\tau$ jets with $P_\tau = +1$, while there may be occasionally a 3rd $\tau$ jet with any polarization (inclusive $\tau\tau$ channel). We shall neglect the contribution from this 3rd $\tau$ to the signal cross-section for simplicity, which means a marginal underestimation of the signal. The raw cross-sections for $\tilde{W}_1\tilde{Z}_2$, $\tilde{W}_1\tilde{W}_1$ and $\tilde{\tau}\tilde{\tau}$ production processes are 770, 850 and 40 fb respectively. We impose the following cuts:

$$p_T^{\tau-\mathrm{jet}} > 15 \text{ GeV},\ \not{E}_T > 20 \text{ GeV},\ |\eta_{\tau-\mathrm{jet}}| < 2.5,$$

$$30^\circ < \phi_{\tau\tau} < 150^\circ,\ \phi_{\not{E}_T\tau} > 20^\circ,\ M_{\tau\tau} > 30 \text{ GeV and } \neq M_Z \pm 30 \text{ GeV}, \tag{12}$$

where we have reconstructed the invariant mass of the $\tau$-pair for the signal and background events after resolving the $\not{E}_T$ into their respective directions. The resulting signal and background cross-sections are listed in Table 3.

We see from the 1st row of Table 3 that the potentially large background from $(Z^\star/\gamma^\star)j$ can be effectively suppressed by the combination of $\not{E}_T, \phi$ and $\tau\tau$ invariant mass cuts in eq. (12). However the $Wj$ background, with the jet faking as a $\tau$, remains about 5 times larger than the $\tau\tau$ signal. In view of the importance of this background we have estimated it via the on-shell $Wj$ as well as the 3-body production processes $q'\bar{q}(g) \to \tau\nu g(q)$ using the matrix elements from [15]. The two estimates agree to within 5%.

Table 3. The signal and background cross-sections (in fb) in the $\tau\tau$ channel after the cuts of eq. (12), including a 50% efficiency factor for each $\tau$ along with a 0.5% probability for mistagging a normal hadron jet as $\tau$. The last row shows the total signal and background cross-sections after the $R > 0.8$ cut on the two $\tau$-jets.

| Signal | | | Background | | | |
|---|---|---|---|---|---|---|
| $\tilde{W}_1\tilde{Z}_2$ | $\tilde{W}_1\tilde{W}_1$ | $\tilde{\tau}\bar{\tilde{\tau}}$ | $Wj$ | $(Z^\star/\gamma^\star)j$ | $WW$ | $t\bar{t}$ |
| 8 | 8.7 | 0.5 | 80 | 2 | 1.7 | 1.2 |
| | 3.5 | | | 3.6 | | |

Fig. 2 compares the $P_\tau = +1$ signal and this $P_\tau = -1$ background as functions of the $\tau$-jet momentum fraction $R$ carried by the charged prong. It clearly shows the complimentary shapes of the two distributions, similar to those of Fig. 1. It means that the difference comes mainly from the opposite polarizations of $\tau$ rather than kinematic difference between the signal and the background. Requiring the charged track to carry $> 80\%$ of the $\tau$-jet energy-momentum ($R > 0.8$) retains 45% of the signal as against only 20% of the background. Moreover the $R > 0.8$ cut is also known to reduce the fake background from normal hadron jets by at least a factor of 5 [16]. Thus demanding both the $\tau$-jets to contain hard charged tracks, carrying $> 80\%$ of their momenta, would reduce the signal by a factor of 5 while reducing the dominant background by at least a factor of 25. The $\tau\tau$ background from $WW$ and $t\bar{t}$ are also reduced by a factor of 25 each. On the other hand the background from $Z^\star/\gamma^\star \to \tau\tau$ has $P_\tau = 0$, and the corresponding distribution lies midway between those of $P_\tau = \pm 1$. The resulting suppression factor is $\simeq (1/3)^2$.

As we see from the bottom row of Table 3 the $R > 0.8$ cut on both the $\tau$-jets reduces the total background to the signal level, i.e. about 3.5 fb each. With the expected Run-2 luminosity of 2 fb$^{-1}$ per experiment, one expects a combined yield of $\sim 14$ signal events against a similar background from CDF and DØ. Note that the corresponding significance level is $S/\sqrt{B} \simeq 4$ with or without the $R > 0.8$ cut. Nonetheless it is no mean gain that this cut can enhance the signal to background ratio from 1/5 to at least 1. This means that the $\tau\tau$ channel can offer a viable SUGRA signature along with the $\ell^+\ell^-\tau$ channel at the Tevatron upgrades, starting with Run-2. It may be noted from Table 3 that requiring the $\tau$ pair to have opposite sign (same

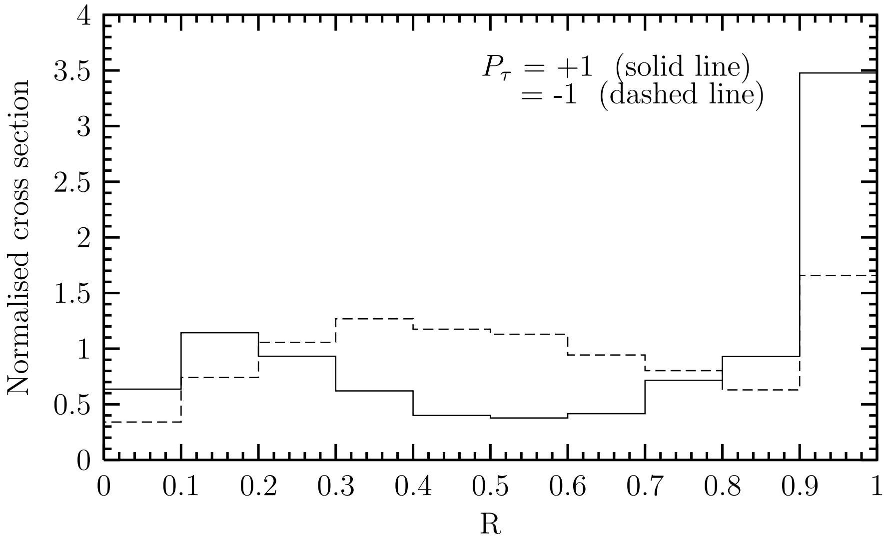


Figure 2: *The normalised SUSY signal* ($P_\tau = +1$) *and* $Wj$ *background* ($P_\tau = -1$) *cross-sections in the 1-prong hadronic* $\tau$*-jet channel shown as functions of the* $\tau$*-jet momentum fraction (R) carried by the charged prong.*

sign) will retain a little over 3/4 (under 1/4) of the signal while retaining 1/2 of the dominant background. Thus with sufficient luminosity it may be possible to improve the signal to background ratio by requiring the $\tau$ pair to have opposite sign. Finally it should be noted that while we have focussed the current analysis on the SUGRA model the same polarization strategy can be used to distinguish the SUSY signal from the SM background in the gauge mediated SUSY breaking model [17], where one expects a $P_\tau = +1$ from the $\tilde{\tau}_R \to \tau\tilde{G}$ decay.

We are grateful to Dhiman Chakraborty, Daniel Denegri and especially Manuel Drees for many helpful discussions. DPR acknowledges partial financial support from IFCPAR.

# References

[1] Review of Particle Properties, Euro. Phys. J. C15, 1 (2000).

[2] H. Baer, M. Drees, F. Paige, P. Quintana and X. Tata, Phys. Rev. D61, 095007 (2001).

[3] H. Baer, C. Chen, M. Drees, F. Paige and X. Tata, Phys. Rev. Lett. 79, 986 (1997); Phys. Rev. D58, 075008 (1998); Phys. Rev. D59, 055014 (1999).

[4] K.T. Matchev and D.M. Pierce, Phys. Rev. D60, 075004 (1999); J.D. Lykken and K.T. Matchev, Phys. Rev. D61, 015001 (2000).

[5] V. Barger, C. Kao and T. Li, Phys. Lett. B433, 328 (1998); V. Barger and C. Kao, Phys. Rev. D60, 115015 (1999).

[6] S. Raychaudhuri and D.P. Roy, Phys. Rev. D52, 1556 (1995); D53, 4902 (1996).

[7] D.P. Roy, Phys. Lett. B459, 607 (1999).

[8] J.H. Kuhn and A. Santamaria, Z. Phys. C48, 445 (1990).

[9] B.K. Bullock, K. Hagiwara and A.D. Martin, Phys. Rev. Lett. 67, 3055 (1991); Nucl. Phys. B395, 499 (1993).

[10] H. Baer, F. Paige, S.D. Protopopescu and X. Tata, hep-ph/0001086.

[11] M. Nojiri, Phys. Rev. D51, 6281 (1995).

[12] CDF Collaboration: F. Abe et. al., Phys. Rev. Lett. 79, 3585 (1997); M. Hohlmann, preprint Fermilab-conf-98-376-E.

[13] M. Hohlmann, Univ. of Chicago, Ph.D. Thesis (1997).

[14] MADGRAPH, T. Stelzer and W.F. Long, Comp. Phys. Commun. 81, 357 (1994); HELAS by H. Murayama, I. Watanabe and K. Hagiwara, KEK-91-11 (1992).

[15] V. Barger and R.J.N. Phillips, Collider Physics, Addison-Wesley (1987).

[16] R. Kinnunen and D. Denegri, CMS Note 1999/037; and private communication from D. Chakraborty and D. Denegri.

[17] D.A. Dicus, B. Dutta and S. Nandi, Phys. Rev. D56, 5748 (1997); B. Dutta, D.J. Muller and S. Nandi, Nucl. Phys. B544, 451 (1999).